Global and Planetary Change 181 (2019) 102999

Contents lists available at ScienceDirect

Global and Planetary Change

journal homepage: www.elsevier.com/locate/gloplacha

Research article

Mountain glacier-to-rock glacier transition

Darren B. Jones[a,*], Stephan Harrison[a], Karen Anderson[b]

[a] College of Life and Environmental Sciences, University of Exeter, Penryn Campus, Penryn, Cornwall TR10 9EZ, UK
[b] Environment and Sustainability Institute, University of Exeter, Penryn Campus, Penryn, Cornwall TR10 9EZ, UK

ARTICLE INFO

Keywords:
Rock glacier
Debris-covered glacier
Transitional processes
Clast form
Transport pathways
Landscape continuum

ABSTRACT

In many of the world's high mountain systems, glacier recession in response to climate change is accompanied by a paraglacial response whereby glaciers are undergoing a transition to rock glaciers. We hypothesise that this transition has important implications for hydrological resources in high mountain systems and the surrounding lowlands given the insulating effects that debris cover can have on glacier ice. Despite this, however, little is known about how this transition occurs nor how quickly, which glaciers are liable to transition, the factors driving this process and the water supply implications that follow. This paper assesses the role of glacier and rock glacier textural properties from a deglaciating region of the Himalayas to begin to address some of these issues. We investigated six landsystems on the spectrum from glaciers-to-rock glaciers in the Khumbu Himal, Nepal, and sampled for clast shape and roundness during 2016 and 2017. Kite aerial photography was additionally used to capture aerial images of an ongoing glacier-to-rock glacier transitional landform (Chola Glacier) to elucidate the surface geomorphic features of a fully transitioned landform. This image data, processed using a structure-from-motion multi-view stereo photogrammetry approach, revealed the presence of a spatially coherent ridge-and-furrow surface morphology in the lower reaches of Chola Glacier, which is potentially indicative of an ongoing glacier-to-rock glacier transition. We show that glacier-derived and slope-derived clast roundness significantly statistically different (Kolmogorov–Smirnov two-sample test: $D_{max} = 0.62$, two-tail $p < .001$; $n = 1650$) and suggest that sediment connectivity (i.e. linkage between sediment sources and downslope landforms) is one of the drivers of the transition process. Consequently, we hypothesise that the presence of well-developed lateral moraines along glacier margins serves to reduce this connectivity and thus the likelihood of glacier-to-rock glacier transition occurring. Understanding such processes has implications for predicting the geomorphological evolution of deglacierizing mountains under future climate warming and the water supply consequences that follow.

1. Introduction

In deglacierizing mountains, the importance of paraglacial (i.e. landscape relaxation) processes, e.g., large-scale rock slope failures and localised rockfalls, are increasingly recognised (Ballantyne, 2002; Harrison, 2009; McColl, 2012; Knight and Harrison, 2014; Beniston et al., 2018). In response to deglacial unloading or debuttressing following the exposure of glacially steepened rockwalls by glacier downwastage and/or retreat (Ballantyne, 2002; Fischer et al., 2006), rock slope modification may subsequently increase supraglacial debris coverage and thickness (e.g., Hambrey et al., 2008; Scherler et al., 2011; Rowan et al., 2015). Continuous and thick (i.e. decimetres to metres) supraglacial debris cover can suppress ablation of the underlying ice (Lambrecht et al., 2011; Pellicciotti et al., 2014) and also influence glacier dynamics significantly. One consequence of this is an increased likelihood that debris-covered glaciers will transform to rock glaciers (Shroder et al., 2000; Jones et al., 2018b; Knight et al., 2019). Given the potential water volume equivalent (WVEQ) stored within rock glaciers around the world (Jones et al., 2018a), and that rock glaciers are reportedly more climatically resilient than debris-free and debris-covered glaciers (Anderson et al., 2018), glacier-rock glacier interactions – e.g., large glacier-rock glacier composite features, comprising debris-covered glaciers in their upper parts and rock glaciers in their lower parts – could enhance the resilience of the mountain cryosphere and preserve frozen water stores in the context of future climate change (Rangecroft et al., 2013; Monnier and Kinnard, 2017; Jones et al., 2018a; Jones et al., 2019). Importantly, the water supply implications associated with rock glacier hydrological contributions under climate change scenarios is yet to be established, with few existing studies investigating this issue (for reviews see: Duguay et al., 2015; Jones et al., 2019).

* Corresponding author.
E-mail address: dj281@exeter.ac.uk (D.B. Jones).

https://doi.org/10.1016/j.gloplacha.2019.102999
Received 10 December 2018; Received in revised form 23 July 2019; Accepted 26 July 2019
Available online 27 July 2019

Improved understanding of glacier-rock glacier interactions, therefore, is of critical importance if we are to better understand the response of high mountain glacial systems to climate change. In addition, there are considerable gaps in understanding whether glaciers will transition to rock glaciers (and develop climatically-resilient water stores) or recede and form lakes dammed by terminal moraines (and potentially produce damaging glacial lake outburst floods).

Found ubiquitously in high mountain systems around the world (see Jones et al., 2018a), rock glaciers are lobate or tongue-shaped assemblages of ice-supersaturated debris and/or pure ice, which slowly creep downslope (see Martin and Whalley, 1987; Barsch, 1996; Haeberli et al., 2006; Berthling, 2011). They typically display rates of movement in the order of centimetres-decimetres per year (see Table 3 in Janke et al., 2013); however, examples of rock glaciers with annual surface velocities of several metres have been reported (Gorbunov et al., 1992; Kääb et al., 2003; Krainer and Mostler, 2006; Delaloye et al., 2013; Sorg et al., 2015; Hartl et al., 2016; Eriksen et al., 2018). They are characterised by distinctive flow-like morphometric features; e.g., spatially organised transverse and longitudinal ridge-and-furrow surface patterns, steep ($\sim >$ 30–35° – gradients of > 40° have been observed [Krainer et al., 2012]) and sharp-crested frontal and lateral slopes etc. (Wahrhaftig and Cox, 1959; Baroni et al., 2004; Kääb and Weber, 2004). Recent research efforts have provided insights into the spatial distribution of rock glaciers (e.g., Jones et al., 2018a, and references therein), internal structure (Hausmann et al., 2007, 2012; Maurer and Huack, 2007; Monnier and Kinnard, 2013, 2015a; Florentine et al., 2014; Emmert and Kneisel, 2017), dynamic behaviour (Kääb et al., 2007; Delaloye et al., 2008, 2010; Serrano et al., 2010; Müller et al., 2016; Wirz et al., 2016; Kenner et al., 2017) and hydrological importance (Azócar and Brenning, 2010; Rangecroft et al., 2015; Janke et al., 2017; Jones et al., 2018a, 2018b). However, the temporal and spatial evolution of glacier-rock glacier interactions remains poorly understood (Monnier and Kinnard, 2015b).

Here, it is important to differentiate rock glaciers from debris-covered glaciers which, in spite of their semantic connection, constitute distinct landforms (Hambrey et al., 2008; Benn and Evans, 2010; Cogley et al., 2011; Kirkbride, 2011). The latter are glaciers partially or wholly covered with a thin (typically less than several-decimetres thick) debris mantle and characterised by a topographically complex, spatially-chaotic mosaic of surficial features, including hummocks, depressions, supraglacial melt ponds and frequent ice exposures (e.g., ice cliffs). Rock glaciers and debris-covered glaciers also have distinct flow dynamics; the former moves as a consequence of internal deformation, which predominantly occurs in a shear zone at depth within the feature (Arenson et al., 2002; Buchli et al., 2013, 2018; Krainer et al., 2015; Kenner et al., 2017), whereas movement of the latter is governed by internal deformation, basal sliding and soft bed deformation (Bosson and Lambiel, 2016). It is worth noting that basal sliding is generally non-occurring or very limited for cold-based debris-covered glaciers (i.e. glaciers frozen to their beds), and only debris-covered glaciers underlain by a soft deformable substrate (i.e. unlithified sediments or poorly consolidated sedimentary rocks) experience soft bed deformation. Nevertheless, glacier-rock glacier interactions have defined the long-standing debate regarding rock glacier origin and evolution that abounds in the literature (see Barsch, 1977, 1987, 1996; Whalley and Martin, 1992; Hamilton and Whalley, 1995; Clark et al., 1998; Whalley and Azizi, 2003; Haeberli et al., 2006; Berthling, 2011). These divergent opinions, termed *the rock glacier controversy* by Berthling (2011), can be framed as the *permafrost model* vs. the *glacier ice-core model*, whereby rock glacier internal ice is assumed to be of a dominantly periglacial/permafrost origin (Wahrhaftig and Cox, 1959; Barsch, 1977, 1987, 1988, 1996; Haeberli, 1985) or glacigenic origin (Outcalt and Benedict, 1965; Potter, 1972; Whalley, 1974; White, 1976; Humlum, 1996; Potter et al., 1998; Ishikawa et al., 2001; Monnier et al., 2013; Petersen et al., 2016; Guglielmin et al., 2018), respectively.

Monnier and Kinnard (2017) have identified three types of glacier-rock glacier interactions within the literature:

(i) Type I: glacier or debris-covered glacier re-advance and subsequent superimposition/embedding onto/into older permafrost bodies (Lugon et al., 2004; Haeberli, 2005; Ribolini et al., 2007, 2010; Monnier et al., 2013; Dusik et al., 2015; Bosson and Lambiel, 2016; Kellerer-Pirklbauer and Kaufmann, 2018; Kenner, 2019) – defined by the *permafrost model*.

(ii) Type II: the continuous emergence of a rock glacier from a debris-covered glacier by evolution of the surface morphology, together with the creep of a massive and continuous ice body that has been buried and preserved (Potter, 1972; Potter et al., 1998; Humlum, 2000; Krainer and Mostler, 2000; Berger et al., 2004; Krainer et al., 2010; Krainer et al., 2012) – defined by the *glacier ice-core model*.

(iii) Type III: debris-covered glacier-to-rock glacier evolution through the transformation of both the surface morphology and the internal structure, i.e. the development of a perennially frozen ice-debris mixture formed via incorporation of surface-derived debris and periglacial ice and fragmentation of the initial massive and continuous ice body (Monnier and Kinnard, 2015b; Seppi et al., 2015; Monnier and Kinnard, 2017). Numerical models of debris-covered glaciers have shown that (iii) forms a plausible end-member response for glacier-rock glacier interactions (Anderson et al., 2018). This has been described as an alternative to the dichotomous debate between a periglacial/permafrost origin or glacigenic origin for rock glaciers (Monnier and Kinnard, 2015b).

  (a) Regarding Type II and III glacier-rock glacier interactions, continuity of the debris-covered glacier and emerging rock glacier morphology suggests a continuum between debris-free glaciers and rock glaciers where debris-covered glaciers form an intermediate stage (Giardino and Vitek, 1988). Striking examples of large, *ongoing* debris-covered glacier-rock glacier transitions are reported in the literature (Shroder et al., 2000; Monnier and Kinnard, 2015b; Monnier and Kinnard, 2017), and these real-world examples alongside numerical modelling simulations (Anderson et al., 2018) indicate that debris-covered glacier-to-rock glacier transitions can occur rapidly (< 100 years). Yet, proponents of the *permafrost model* and *glacier-ice core model* have generally orientated studies towards already well-developed landforms (Monnier and Kinnard, 2015b).

Consequently, there exists an opportunity to conduct research that addresses questions about the processes governing *ongoing* debris-covered glacier-to-rock glacier transitions in order to elucidate the drivers that determine the likelihood that this transition will occur (Jones et al., 2019). Answering this question is of great importance if we wish to understand how glaciated mountains might evolve with future climate change, and the hydrological and water supply implications that follow (ibid.). To illustrate this issue our study focuses upon an exemplar region where glaciers (clean and debris-covered) and rock glaciers co-exist to: (i) investigate the sedimentological and geomorphological characteristics associated with a range of relevant landforms; and (ii) develop a hypothesis for glacier-to-rock glacier transition.

2. Regional setting

2.1. Climatological and geological context

The study area is located in the Sagarmatha National Park (SNP), Khumbu Himal, north-eastern Nepal (Fig. 1a). The climate of this area is dominated by the South Asian Summer Monsoon, with data from the PYRAMID Observatory Laboratory (hereafter: PYRAMID) near Lobuche (5035 m a.s.l.) indicating that 90% of annual precipitation falls during June–September (Bollasina et al., 2002; Salerno et al., 2015). Also, instrumental records reflect a topographically-driven steep

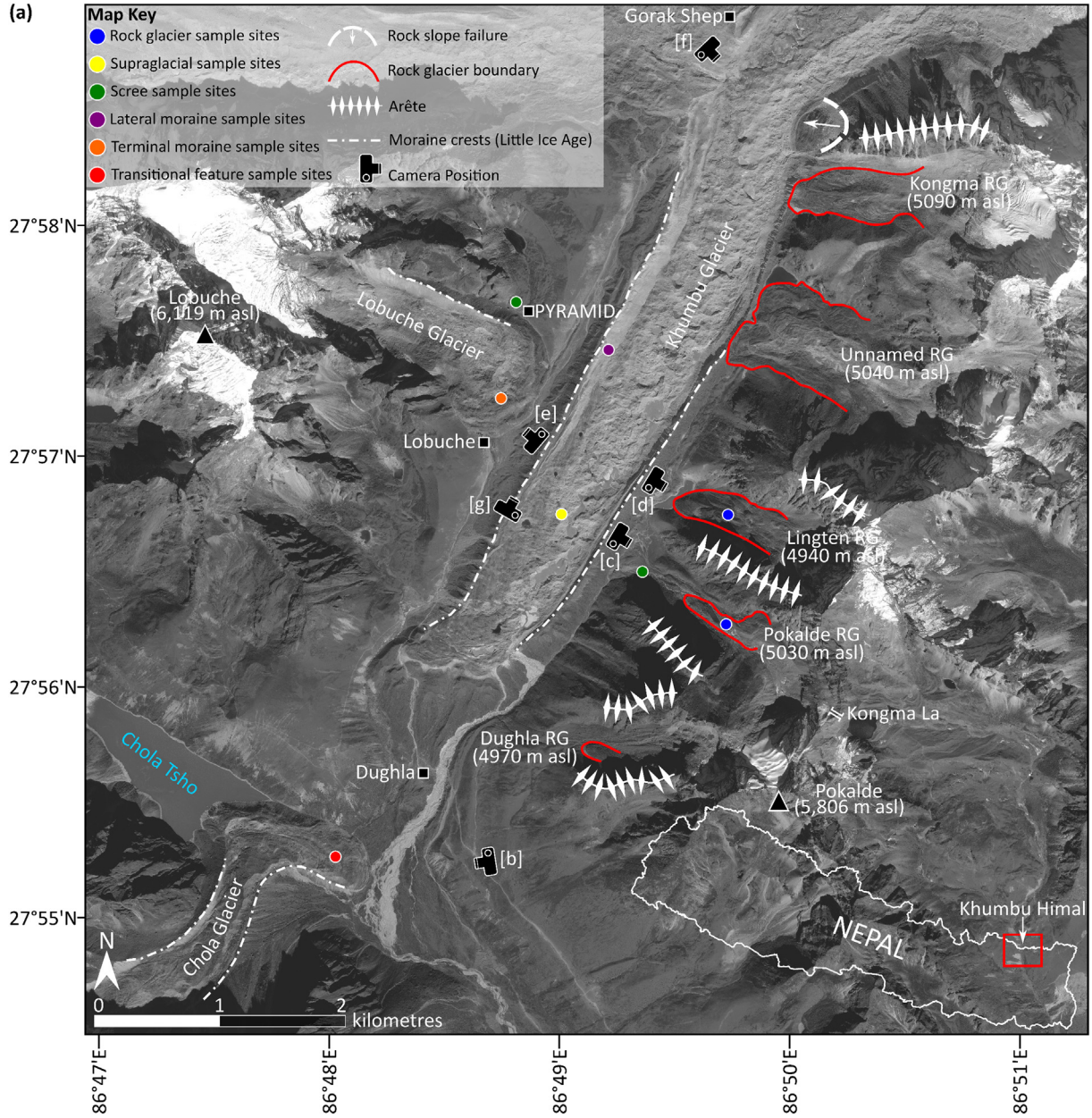

Fig. 1. (a) The spatial distribution of relevant geomorphological landforms situated within the Khumbu valley and discussed in this paper. Sampling sites for clast characteristic analysis are indicated. Values (m asl) reflect the elevation of rock glacier (RG) termini. Background: orthorectified Pleiades panchromatic scene from November 2016. Inset: the location of the Khumbu Himal in Nepal. Annotated photographs of selected geomorphological elements examined in this paper are indicated: (b) Chola Glacier, probably undergoing contemporary glacier-rock glacier transition; (c) Pokalde rock glacier (glacier-derived); (d) Lingten rock glacier (glacier-derived); (e) debris-mantled surface and terminal moraine of Lobuche Glacier; (f) examples of rock slope failure, LIA moraine collapse and evidence for the degree of glacier downwasting below the LIA trimline; and (g) right-lateral moraine of Khumbu Glacier (photos: D.B. Jones [b-d, f] and O. King [e, g]).

precipitation gradient, with a pronounced south (Chaurikharka [~2600 m a.s.l.]: 2418 mm yr^{-1}) to north (PYRAMID: 449 mm yr^{-1}) reduction in precipitation within the SNP (Salerno et al., 2015). Mean annual air temperature at the PYRAMID (1994–2012) was −2.4 °C, and mean temperature above 5000 m a.s.l. is increasing by 0.044 °C yr^{-1} (ibid.). Seismic refraction studies conducted on four rock glaciers in the study region indicate that the regional lower limit of discontinuous permafrost is situated at ≃5000–5300 m a.s.l. (Jakob, 1992); however, ice preservation in openwork block debris accumulations (e.g., rock glaciers) several hundreds of metres below the regional limit of discontinuous permafrost have been reported (e.g., Delaloye and Lambiel, 2005). The detailed bedrock geology of the Everest Massif has been described (see Searle et al., 2003). Of significance for this study is that the features studied in this paper have surface debris consisting predominantly of granitic and gneissic debris, with some migmatitic debris. In the Khumbu region numerous landforms from across the spectrum of the glacial-paraglacial-periglacial landscape continuum occur within a relatively small spatial area. This means that climate conditions are relatively homogenous in the area and that we can therefore better isolate the non-climatic processes driving glacier-to-rock glacier transition.

2.2. Geomorphological context of debris-mantled landforms

The ~15.7 km long Khumbu Glacier (27°56′N, 86°49′E; Fig. 1a) flows from the Western Cwm between Mt. Everest (8848 m a.s.l.), Mt.

Fig. 1. (*continued*)

Lhotse (8516 m a.s.l.) and Mt. Nuptse (7861 m a.s.l.) via the Khumbu Icefall, and terminates at ~4900 m a.s.l. The lowermost ~8 km is debris-mantled, with debris thickness increasing towards the glacier terminus and reaching several metres (Nakawo et al., 1986). The debris-covered glacier tongue is characterised by a very low gradient, with the lowermost 3–4 km believed to be flowing at velocities < 10 $m{\cdot}a^{-1}$ (i.e. stagnant) (Hambrey et al., 2008; Quincey et al., 2009), and a pair of prominent lateral moraines (Fig. 1a and g) dating from the Little Ice Age (LIA) (Rowan, 2017). Lobuche Glacier (Fig. 1a and e) on the western side of Khumbu Glacier is smaller and encompasses a relic debris-mantled ablation zone ~1 km in length that is disconnected from the clean-ice accumulation zone (Watson et al., 2018). Chola Glacier (Fig. 1a and b), believed to be a glacier-rock glacier composite landform (Knight et al., 2019), is located beneath Mt. Taboche (6542 m a.s.l.) and Mt. Cholatse (6440 m a.s.l.) and flows ~3 km to ~4400 m a.s.l. It is characterised by large, asymmetrical lateral moraines and has a near-continuous debris-mantle over the entirety of its length. Lastly, rock glaciers have been extensively mapped across the Khumbu Himal (Regmi, 2008; Jones et al., 2018b), including a number situated within the Pokalde Massif on the eastern side of Khumbu Glacier. In the field, Lingten and Pokalde rock glaciers were investigated in detail. Both of these are glacier-derived rock glaciers, and thus of glacigenic origin (Knight et al., 2019). The main properties of these rock glaciers, such as their sediment budget and general characteristics, have been examined in previous studies (Barsch and Jakob, 1998; Knight et al., 2019). Pokalde rock glacier is located at ~5030 m a.s.l. with a west-facing aspect. It has a relatively flattened body and gently sloping front of < 30°, with minor vegetation and lichen cover (Fig. 1c). Knight et al. (2019) suggest that this rock glacier is inactive (i.e. containing ice but immobile). Pokalde Glacier, located immediately upslope of this rock glacier, has receded considerably in recent years. Lingten rock glacier is located at ~4940 m a.s.l. and extends from talus slopes beneath a high (~400–500 m), steep headwall (Fig. 1d). The rock glacier has a steep (> 30–35°), high (> 30–40 m) and sharp-crested frontal slope, light-coloured frontal slope, and no vegetation cover; characteristics that indicate the upper lobes contain frozen material and are seasonally active (Knight et al., 2019). Conversely, the lowermost lobe has extensive vegetation cover with boulders that are weathered and lichen-covered, indicating long-term stability (i.e. the rock glacier contains no ice and is immobile [relict activity status]) (ibid.).

3. Methods

3.1. Clast morphology

Paraglacial landscapes represent highly dynamic systems; the adjustment from glacial- to paraglacial-dominated process regimes in high mountain systems occurs over a range of timescales. Therefore, "[g]eoscientists [and geomorphologists] are generally unable to fully observe landscape forming processes because the time-scale of the observer and the time-scale of many geomorphic phenomena are different" (Micallef et al., 2014). Location-for-time substitution facilitates the inference of long-term landform development based upon the assumption that the modern landscape contains representative landforms at different stages of evolution, the comparison of which enables integration of long-term processes and short-term investigations (field-based "snapshots") (see Paine, 1985) (e.g., Micallef et al., 2014; Klaar et al., 2015; Messenzehl et al., 2017). Previous research has indicated the utility of clast shape and roundness for distinguishing between different erosional, transportational and depositional clast histories in glaciated environments (e.g., Ballantyne, 1982; Benn and Ballantyne, 1993, 1994; Bennett et al., 1997; Hambrey and Ehrmann, 2004; Glasser et al., 2009; Brook and Lukas, 2012; Małecki et al., 2018), thus enabling the creation of hypotheses to test models of landscape development. Here, therefore, we substitute data collected through time with clast data from a range of landforms that span the glacier-rock glacier continuum to elucidate the nature of transitions along this evolutionary pathway.

During two field campaigns undertaken in May 2016 and 2017, 1650 clasts from surface deposits were taken to determine clast shape (i.e. the relative dimensions of the clast) and roundness (i.e. the degree of curvature around the clast edges) characteristics following the method of Benn and Ballantyne (1993, 1994). Sedimentary facies were also described in the field on the basis of Hambrey and Glasser's (2003) modification of Moncrieff's (1989) textural classification of poorly sorted sediments. Field sampling was undertaken at 33 sites located across six distinct morphometric features on and in the vicinity of the Khumbu Glacier (Fig. 1a; Table 1): supraglacial debris, terminal moraine debris, lateral moraine debris, rock glacier debris, possible glacier-rock glacier composite landform debris (termed: transitional feature) and rockfall debris (termed: scree). The clasts, in groups of fifty, were selected at random from 2 m^2 sample sites and the three orthogonal axes *a, b, c* (long, intermediate, short) were measured to the nearest 5 mm using a steel ruler. Clast roundness was determined visually for each clast on a modified Powers (1953) scale. Given the potential influence of lithology in determining clast shape (see Lukas et al., 2013), we confined our sampling strategy to clasts of similar lithology (granitic gneiss).

As advocated by Benn and Ballantyne (1993, 1994), ternary diagrams following Sneed and Folk (1958) were generated in the TRIPLOT Excel spreadsheet (Graham and Midgley, 2000) and employed to visually and statistically interpret clast shape. The C_{40} index (percentage of clasts with a c/a axial ratio ≤ 0.4), was subsequently calculated for each sample site (i.e. 50 clasts). Clast roundness classifications were plotted as frequency distributions (%) and assessed visually. The RA index (percentage of angular and very angular clasts), was then determined for each sample site. Here, the C_{40} and RA indices are assumed to represent two contrasting modes of sediment transport: (i) active transport at or close to the ice-bed interface (i.e. subglacially modified); and (ii) passive transport at the feature surface (i.e. supraglacially transported) or within the ice (i.e. englacially transported) (Boulton, 1978; Benn, 2004). Boulton (1978) showed that dominantly edge-rounded, blocky and abraded clasts occurred in (i) and dominantly angular and platy clasts in (ii). To this end, the co-variance of the RA and C_{40} parameters for the six different morphometric features were plotted on a bivariate scatterplot as suggested by Benn and Ballantyne (1994). Landform associations were further statistically interrogated using the Kolmogorov-Smirnov two-sample test (McCarroll, 2016, p. 132).

3.2. Structure-from-Motion Multi-View Stereo (SfM-MVS) photogrammetry

In addition to sedimentological sampling, an experiment was undertaken to test the utility of emerging structure-from-motion multi-view stereo (SfM-MVS) photogrammetry approaches for modelling the surface features of a potentially ongoing glacier-to-rock glacier transition. Drones have emerged in geomorphological research as a de facto platform for SfM-MVS data capture (Smith et al., 2016), but the use of drones in the study area was not feasible for a number of reasons. The SNP authority operates restrictions regarding the use of drones, which can make obtaining research permits more difficult (D. Regmi [Himalayan Research Expeditions], pers. comm.). Power supply issues, e.g., limited availability of solar power, device-type charging restrictions, high costs (~400 Rs./hr ≈ 3.5 USD) and low air mass – which results in poor flight efficiency and very short flight times – also restricts the use of drones here. In comparison to drones, kite aerial photography (KAP) provides a number of advantages in high-altitude locations (Wigmore and Mark, 2018). These include: (1) KAP platforms are less affected by the lower air density of high-altitude regions; (2) KAP platforms are lighter and more compact than drones and thus simpler to transport to field sites; (3) powerful katabatic winds characteristic of high-altitude environments form conditions suitable for KAP, however, represent hazardous conditions for drones; (4) KAP platforms are less prone to breakage than drones, an important consideration given the complex nature of mountainous terrain and the greater expense of the latter (ibid.).

Aerial images of the Chola Glacier were captured using KAP. A HQ KAP Foil 1.6 m^2 single-line kite was used for this purpose (Fig. 2a); a KAP system previously demonstrated to provide a stable aerial platform (e.g., Duffy et al., 2018). This KAP system is suitable for wind conditions between 3.13 and 13.86 m s^{-1} (KAPshop, 2019). PYRAMID Observatory Laboratory data indicates well-defined local circulatory systems with consistent south-southwest valley breezes (~4.5 m s^{-1}) peaking between 12:00 to 14:00 (Bollasina et al., 2002); therefore, the chosen kite platform was well-suited to these conditions. A ruggedized Canon PowerShot D30 12.1-megapixel compact digital camera was used to capture aerial photographs. The Canon Hack Development Kit

Table 1
Study sample site information. This information is also visualized in Fig. 1a.

Feature name	Latitude	Longitude	Elevation (m a.s.l.)	Facies sampled
Khumbu Glacier	27°56′30″N	86°48′54″E	4950	Supraglacial debris
	27°57′16″N	86°49′07″E	4990	Lateral moraine debris
Lobuche Glacier	27°57′06″N	86°48′42″E	5010	Terminal moraine debris
Pokalde rock glacier	27°56′07″N	86°49′40″E	5190	Rock glacier debris
Lingten rock glacier	27°56′35″N	86°49′44″E	5130	Rock glacier debris
Chola Glacier	27°54′59″N	86°48′00″E	4450	Transitional feature debris
Scree	27°56′18″N	86°49′14″E	4920	Rockfall debris
	27°57′32″N	86°48′44″E	5020	Rockfall debris

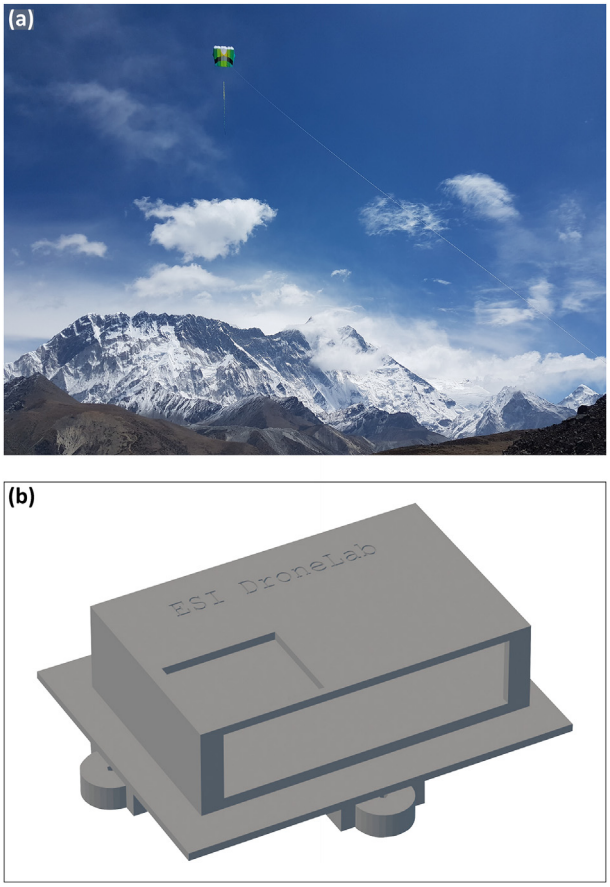

Fig. 2. (a) The KAP system during a test flight on Duwo Glacier beneath Ama Dablam. The Nuptse-Lhotse ridge forms the backdrop. N.B. the larger HQ KAP Foil 5.0 m^2 single line kite is depicted. This KAP system, facilitating KAP in lower wind conditions (1.79–8.94 m s^{-1}) (KAPshop, 2019), was also transported to the field sites but not used; and (b) 3D model representation of the picavet mount (photo: D.B. Jones).

firmware (CDHK; chdk.wikia.com/wiki/CHDK) was loaded onto the SD card, enabling fixed interval shooting; here, an interval of 5 s was used. The camera was mounted on a custom 3D printed lightweight mount (Fig. 2b) and hung from a picavet suspension system ~10 m below the kite. The picavet system uses a system of twine and pulleys that serve to stabilize the KAP platform with the camera facing in the nadir position. In the field, 13 highly visible black and white chequered 250 mm × 250 mm plastic ground control points (GCPs) were distributed along the terminus of Chola Glacier. Laminated sheets with unique identifiers were positioned alongside each GCP to simplify maker identification within the images and the GCP position was measured with a GARMIN eTrex® 10 Handheld GPS. Geospatial data collected from this device were recorded in the WGS-84 datum (ESPG: 4326) with an average horizontal error of ± 3 m. The kite was then walked around the Chola Glacier in a zig-zag fashion to ensure good image overlap and to gather images from various perspectives, both of which are important for the functioning of SfM-MVS algorithms (Westoby et al., 2012).

Through manual inspection KAP-derived aerial images were filtered, removing those with visible motion blur, an excessively oblique angle, non-stationary occlusions such as people, and those captured during take-off and landing. This resulted in a subset of 282 images, which formed the input for a photogrammetric processing workflow. Subsequently, a dense point cloud, digital surface model (DSM) and orthomosaic were built using Agisoft PhotoScan Professional (v. 1.3.5) (Agisoft LLC, 2017). The sequential steps and the settings used within the photogrammetric workflow are available in the supplementary information. The specific algorithms implemented by PhotoScan are not detailed here, however, the SfM-MVS procedure is described by Westoby et al. (2012).

4. Results and discussion

4.1. Analysis of clast sedimentology

Ternary diagrams and roundness histograms for the features sampled in situ are shown in Fig. 3, and the RA-C_{40} (i.e. roundness vs. shape) bivariate scatterplot in Fig. 4.

Sandy boulder-gravel, with minor cobbles and pebbles, dominates the near-continuous debris-mantle in the lower portions of Khumbu Glacier (Fig. 5a). Supraglacial samples have moderate-high c:a ($\tilde{x}$ = 0.50) and b:a ($\tilde{x}$ = 0.78) axial ratios and thus aggregate clast form is predominantly blocky (Ballantyne, 1982). Of note, C_{40} indices range considerably between 6% and 44%, indicating that supraglacial facies also contain smaller proportions of platy/elongate clasts. Typical clast roundness distribution of supraglacial facies reflects the predominance of sub-angular clasts (68%), with lower occurrence of very angular (1%), angular (20%) and sub-rounded (11%) clasts. RA values are generally low (< 20%), however two samples have more moderate values (32–36%). Generally, supraglacial samples are predominantly very angular and/or angular (e.g., Benn and Ballantyne, 1993, 1994; Bennett et al., 1997; Benn and Owen, 2002; Glasser et al., 2009; Brook and Lukas, 2012); thus, here, aggregate clast form attributes of supraglacial samples indicate that most debris has likely undergone active transportation at the ice-bed interface (Boulton, 1978) or fallen from collapsing lateral moraines (Hambrey et al., 2008; Fig. 1f). Additionally, the presence of large sub-angular/sub-rounded boulders up to 5 m (b-axis) at the surface (Fig. 5a) and bullet-nosed clasts (Boulton, 1978; Benn et al., 2004, p. 362) suggests the importance of subglacial transport paths. Hambrey et al. (2008), report similar aggregate clast form results for supraglacial samples on Khumbu Glacier, lending credence to the findings presented above.

The LIA lateral moraines of Khumbu Glacier have unstable, non-vegetated inner faces dominated by sandy-boulder gravel (Fig. 5b). Atop the lateral moraines, large, angular boulders several metres in diameter are present (Fig. 1g). Clasts are blocky with moderate-high c:a ($\tilde{x}$ = 0.50) and b:a ($\tilde{x}$ = 0.75) axial ratios (Ballantyne, 1982). C_{40} (< 20%) and RA indices (< 32%) are both reasonably low (i.e. dominantly blocky shapes and very high percentages of edge-rounded clasts). Furthermore, clasts in lateral moraine facies are predominantly angular, sub-angular and sub-rounded, in which sub-angular and sub-rounded clasts are dominant with up to 64% and 38% in this category, respectively. The co-variant plot demonstrates a narrow distribution of RA/C_{40}, further suggesting a predominantly basal-origin for debris (i.e. actively transported).

Terminal moraine facies, sampled at Lobuche Glacier (Fig. 1a), are predominantly blocky with moderate-high c:a ($\tilde{x}$ = 0.50) and b:a ($\tilde{x}$ = 0.75) axial ratios and few platy/elongate clasts (C_{40} = 24%) (Ballantyne, 1982). Clast roundness distribution is broad, with peaks in the angular (40%) and sub-angular (52%) categories. Additionally, the co-variant plot depicts comparatively high RA indices (38–50%) vs. supraglacial and lateral moraine facies, which combined with the presence of large, angular boulders (Fig. 5c), infers a variable mixture of actively and passively transported sediment.

Scree facies, sampled at a number of locations (Fig. 1a), are categorised as boulder-gravel, with minor proportions of cobbles and pebbles (Fig. 5d). Additionally, angular boulders > 5 m (b-axis) are common at the foot of rockwalls (Fig. 5d). Sampled clasts have low-moderate c:a ($\tilde{x}$ = 0.38) and moderate-high b:a ($\tilde{x}$ = 0.67) axial ratios and thus aggregate clast form is predominantly platy (Ballantyne, 1982). Relatively high C_{40} indices (60% [46–72%]) support this interpretation. Furthermore, clasts are predominantly very angular and angular (53% and 38%, respectively), with minor proportions of sub-

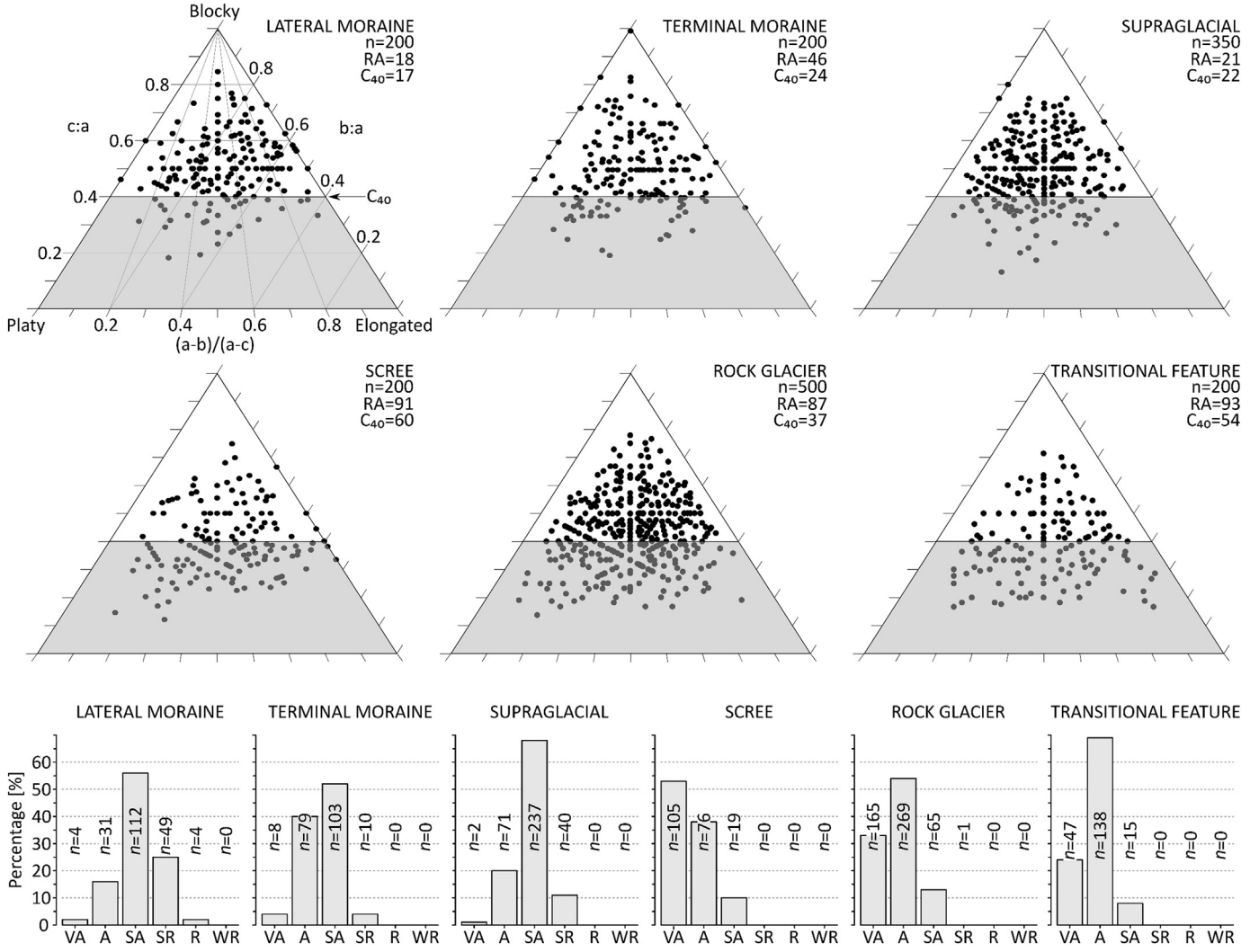

Fig. 3. Aggregate clast shape data (ternary diagrams) and roundness data (histograms) for the six morphometric features. Abbreviations: *n* is the number of clasts sampled; *RA* and C_{40} are defined in the text; *VA* = very angular; *A* = angular; *SA* = sub-angular; *SR* = sub-rounded; *R* = rounded; and *WR* = well-rounded.

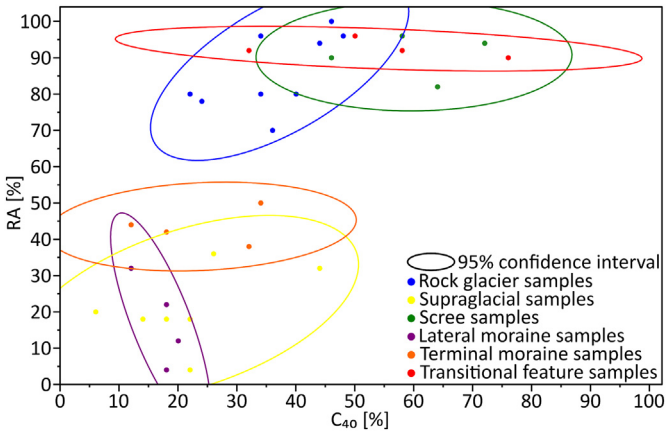

Fig. 4. Summary RA-C_{40} bivariate scatterplot of the features sampled in situ. Envelopes (ellipses) reflect the 95% confidence interval of each data group. Abbreviations: *RA* and C_{40} are defined in the text. N.B. each plotted point represents a sample group of 50 clasts.

angular debris. Intra-sample RA indices are all > 82%. Combined, this indicates that scree facies have undergone predominantly passive transport.

Rock glacier facies are dominated by matrix-free, angular boulder-gravel (Fig. 5e); thus, Pokalde and Lingten rock glaciers can be designated 'bouldery rock glaciers' according to Ikeda and Matsuoka's (2006) classification. In addition, paraglacially driven rockfall, e.g., large, angular rockfall debris several metres in diameter and perched boulders, characterise the rock glacier surface (Fig. 5e). The frontal slope of the rock glaciers is dominated by sandy boulder-gravel, with minor cobbles and pebbles. Sampled clasts have moderate c:a ($\tilde{x}$ = 0.44) and moderate-high b:a ($\tilde{x}$ = 0.71) axial ratios and thus aggregate clast form is a variable mixture of blocky, platy and elongate forms. Moderate C_{40} indices of 37% indicate that platy/elongate clasts form a larger proportion of the total sample compared to supraglacial, lateral moraine and terminal moraine facies. Rock glacier facies are dominated by very angular (33%) and angular (54%) debris, and RA indices are consistently high (87% [70–100%]). Importantly, RA indices of Lingten rock glacier samples (94–100%) are considerably higher than those of Pokalde rock glacier (70–80%). This may indicate that Pokalde rock glacier likely formed via a Type I glacier-rock glacier dynamic relationship, whereas Lingten rock glacier represents a Type II or III glacier-rock glacier dynamic relationship. Therefore, while rock glacier facies data indicates predominantly passively transported sediment, that of Pokalde rock glacier is partially reworked subaerial debris (i.e. has undergone a degree of active transport) (Knight et al., 2019).

Transitional feature facies are classified as predominantly sandy

Fig. 5. Typical facies associated with the morphological units studied here: (a) sandy boulder-gravel on lower Khumbu Glacier; (b) general view of the right-lateral moraine showing sandy boulder-gravel, with large boulders atop the crest; (c) boulder-gravel, including large, angular boulders; note the GCP target for scale; (d) boulder-gravel, with minor proportions of cobbles and pebbles, characterising the scree slopes below Pokalde rock glacier. Large, angular debris in the foreground and smaller debris in the background suggesting a degree of fall sorting; (e) paraglacially driven rockfall (i.e. very large, angular debris) upon Lingten rock glacier; note the sandy boulder-gravel with minor cobbles and pebbles forming the frontal slope of the rock glacier in the background; and (f) matrix-free boulder-gravel at the surface of Chola Glacier. Large, angular boulders resulting from rockfall are evident at the surface (photos: D.B. Jones).

boulder-gravel, with minor cobbles and pebbles. Transitional feature facies within the furrows in particular, are predominantly matrix-free boulder-gravel, with minor cobbles and pebbles and lacking significant sand. Similar to scree and rock glacier facies, transitional feature facies have low-moderate c:a ($\tilde{x}$ = 0.40) and moderate-high b:a ($\tilde{x}$ = 0.71) axial ratios, indicating that aggregate clast form is predominantly platy (Ballantyne, 1982). Clast roundness distribution reflects the predominance of very angular (69%) and angular clasts (24%), with lower occurrence of sub-angular (8%) clasts. The co-variant plot show RA/C_{40} indices typically of 93/54 (%). Mean clast size (b-axis) of 30 boulders lying along an upslope transect was ~1.9 m, with several large, angular boulders > 5 m (Fig. 5f). This is indicative of the movement to the snout of rockfall-derived debris (Knight et al., 2019). Together, the above-described characteristics of transitional feature facies infers the dominance of passive transport processes.

The co-variant plot indicates that the sampled sedimentary facies form two groups with no overlapping geometrical properties (Fig. 4): (i) glacier-derived sediment (i.e. predominantly active transport processes), including supraglacial, lateral moraine, and terminal moraine facies; and (ii) slope-derived sediment (i.e. predominantly passive transport processes), consisting of scree, rock glacier and transitional feature facies. A Kolmogorov–Smirnov two-sample test was applied to the data and showed that glacier-derived and slope-derived sediment were significantly statistically different with regard to clast roundness (D_{max} = 0.62, two-tail p < .001; n = 1650).

4.2. Analysis of KAP-derived SfM-MVS products

On Chola Glacier which is a transitional feature we used KAP to produce an SfM-MVS workflow and this yielded a point cloud, DSM

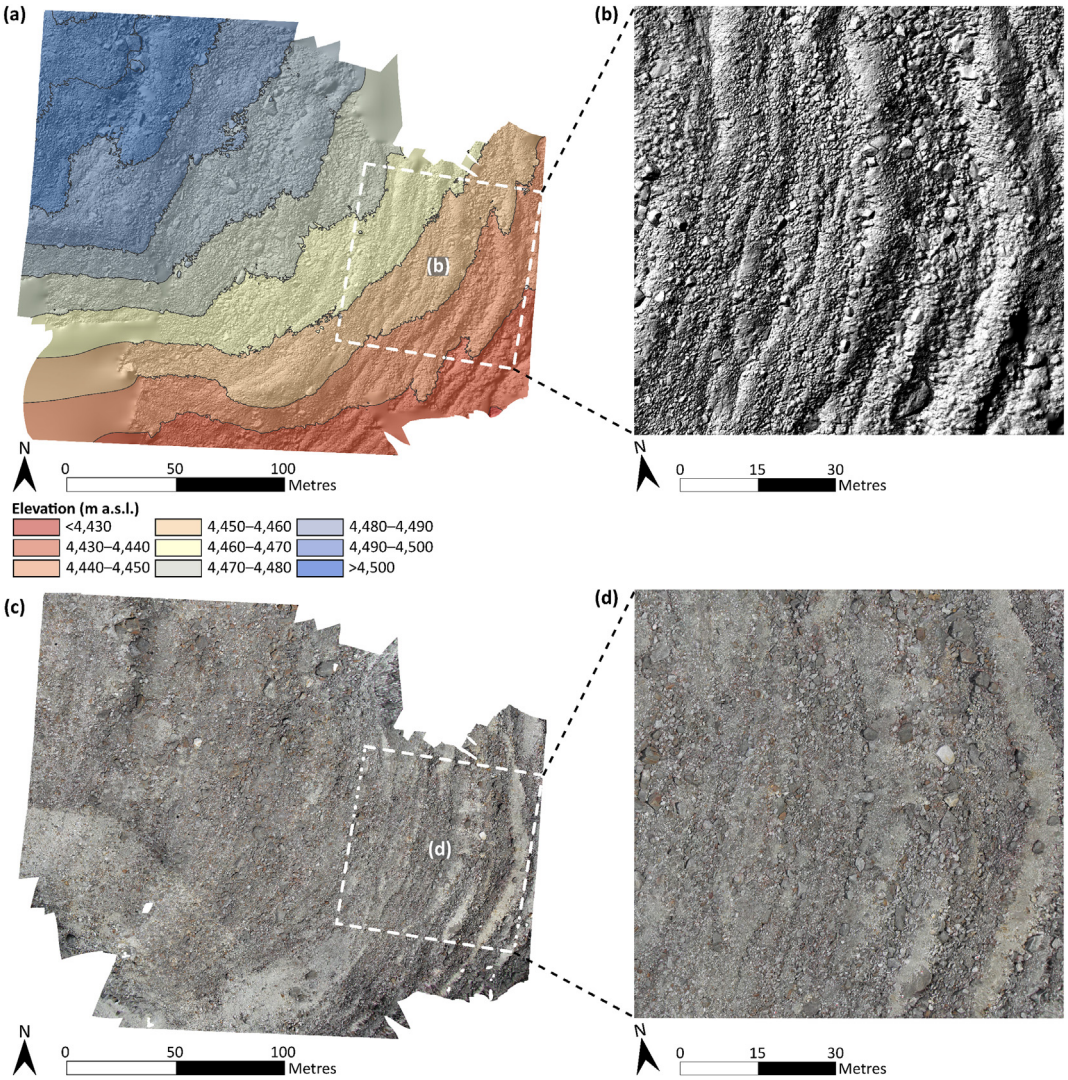

Fig. 6. Products of the SfM-MVS workflow: (a) overview of topography of Chola Glacier, as represented by a hillshaded DSM. Contours at 10 m intervals are also depicted; (b) finer spatial scale overview showing the ridge-and-furrow surface morphology, characteristic of rock glaciers, in the lower parts of the feature. Large boulders several metres in diameter (b-axis) are also visible; (c) overview of the sedimentological facies of Chola Glacier, visible in the orthomosaic. Debris banding reflects the aforementioned ridge-and-furrow surface morphology, with sandy boulder-gravel and boulder-gravel present on the distal and proximal slopes, respectively; and (d) finer spatial scale view of the transitional feature facies upon Chola Glacier. Large, angular boulders that reflect paraglacially driven rockfall evidence are common across the surface.

(Fig. 6a) and orthomosaic (Fig. 6c) covering ~0.04 km^2. The mean flying altitude was 33.2 m. The photogrammetric workflow produced a point cloud with 27.6 points cm^{-2}, a DSM with a ground resolution of 19.00 mm $pixel^{-1}$ and an orthomosaic with a ground resolution of 9.52 mm $pixel^{-1}$. The re-projection error (calculated by the software) was ~0.6 pixels. Note that three of the original GCPs were omitted from the processing workflow for use as independent check points. Root mean square error (RMSE) calculated across x, y and z dimensions was ~5.8 m. The relatively large RMSE is to be expected when spatially variable overlap (typical of KAP surveys), and standard accuracy GPS (from a handheld system) is present. Please see the supplementary information for the full processing report of this model construction. Quantitative analysis of the DSM was not undertaken, instead the focus was on visual interpretation of the model surface, which exhibits the presence of a spatially coherent ridge-and-furrow surface morphology in the lower reaches of Chola Glacier (Fig. 6b). Numerous large, angular boulders > 5 m (b-axis) are present across the surface; further evidence of the movement to the snout of rockfall-derived debris (Fig. 6d). Alongside the sedimentological analyses, this suggests that Chola Glacier potentially represents a contemporary transitional form.

4.3. Synthesis of site-wide variations

The data suggest strongly that the surficial sediments in the lower reaches of Khumbu Glacier are linked to glacier-derived sediment and therefore we argue that the glacier is not transitioning. In contrast, the sediments associated with the lower reaches of Chola Glacier are slope-derived and the glacier represents an ongoing glacier-to-rock glacier transition. Given the importance of debris-supply from bordering valley sides (Benn and Owen, 2002), this suggests a strong link between the delivery of sediment from the surrounding unstable mountain slopes to the glacier surface and the likelihood of glacier-to-rock glacier transition occurring. Indeed, Chola Glacier and the sampled rock glaciers are well connected to their debris source as they are in close proximity to rock-slopes where paraglacial processes occur with a high frequency (i.e. steep and tall rockwalls [amphitheatre-like]). Pokalde rock glacier, which represents a Type I glacier-to-rock glacier transition (Section 1) is less well-connected, and thus is *dynamically inactive* (see Barsch, 1996, p. 8–10) and is transitioning towards relict activity status. It is clear from the data presented here and within other studies (Degenhardt Jr, 2009; Kellerer-Pirklbauer and Rieckh, 2016) that sufficient sediment

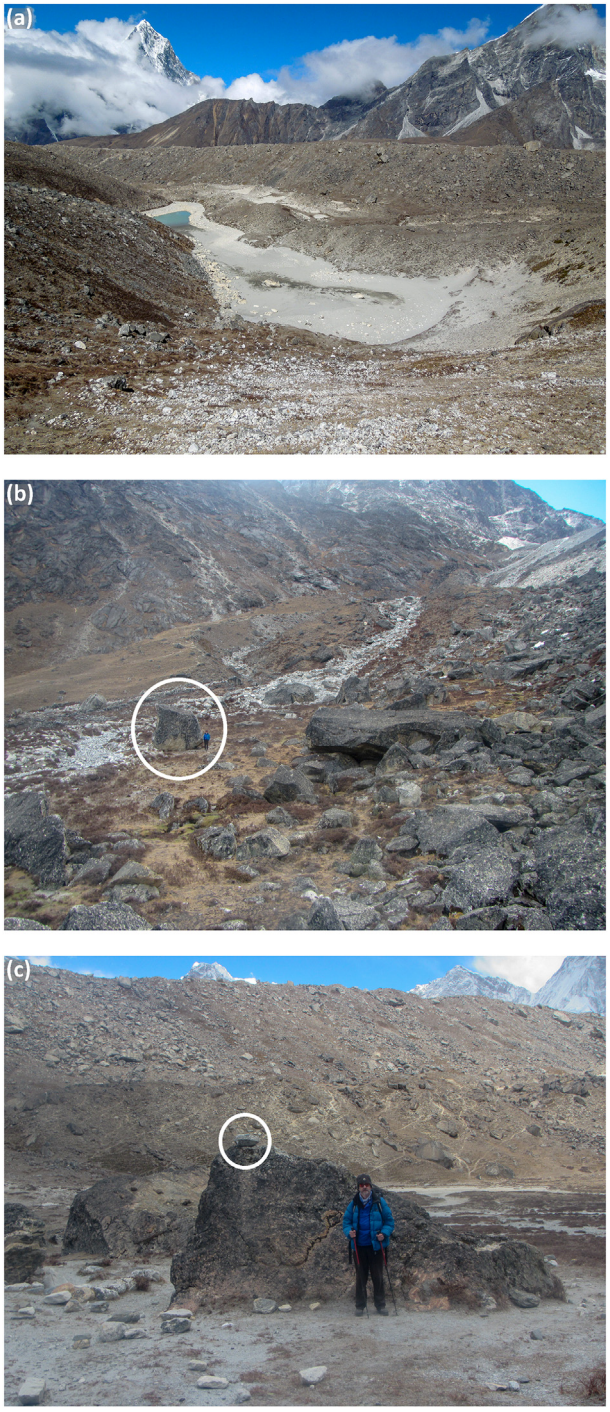

Fig. 7. (a) the lateral morainic trough and LIA left-lateral moraine of Khumbu Glacier; (b) rockfall-derived large, angular boulders that are trapped in the lateral morainic trough; note the encircled person for scale; and (c) view of the LIA left-lateral moraine from within the lateral morainic trough. Further evidence of debris trapped within the lateral morainic trough is depicted; note the encircled perched boulders (photos: D.B. Jones).

supply is critical to rock glacier development and persistence. Therefore, it is reasonable to assume that low sediment connectivity (i.e. linkage between sediment sources and downslope landforms) will reduce the likelihood with which glacier-to-rock glacier transition occurs.

As a result, we hypothesise that sediment delivery to the glacier surface is an important (and perhaps the primary) driver of glacier-to-rock glacier transition. The sedimentological facies of Khumbu Glacier vs. Chola Glacier (and the rock glaciers) have undergone significantly different transport processes. The predominance of glacier-derived sediment (i.e. actively transported sediment) that characterises Khumbu Glacier indicates that the lower reaches of the glacier are not influenced by paraglacial processes. As significant rockfall input is arguably the most efficient way for glacier-to-rock glacier transition to occur, we hypothesise that the large, well-developed lateral moraines of Khumbu Glacier, the trough-to-crest height of which is 75 m (left) and 60 m (right) in the vicinity of Lobuche (Hambrey et al., 2008; Fig. 1a), blocks the sediment from rockfalls reaching the glacier surface (Fig. 7a). Furthermore, the Khumbu Valley widens with distance downslope and the surrounding slopes are also elevationally lower. There is plentiful evidence of paraglacially driven rockfall at the base of slopes in the lateral morainic troughs alongside Khumbu Glacier; however, much of this debris becomes trapped here (Fig. 7b and c). That is not to say that glaciers with large, well-developed lateral moraines will not undergo glacier-to-rock glacier transition, but they may require catastrophic events (e.g., sturzstrom) to facilitate this. Therefore, the ice-debris ratio (debris concentration) of Khumbu Glacier is such that while the terminus shows features (e.g., ridge-and-furrow surface morphology) characteristic of rock glaciers (Iwata, 1976; Fig. 1a), the lack of sufficient sediment delivery indicates that Khumbu Glacier is following a trajectory towards large supraglacial lake formation dammed by an ice-cored terminal moraine, in agreement with previous research (e.g., Hambrey et al., 2008; Watson et al., 2016). Furthermore, Monnier and Kinnard (2017) note that rock glaciers can develop upward at the expense of debris-covered glaciers, and this cannot occur on Khumbu Glacier if a large supraglacial lake forms.

5. Conclusion

Here we have used location-for-time substitution to investigate clast data from a range of landforms that span the glacier-rock glacier continuum in a high mountain setting to assess the ways in which glacier-to-rock glacier transition occurs. We can show clear sedimentological differences in these landforms and suggest that access to debris supply is one of the drivers of the transition process. As a result, the topographic connectivity between glacier surfaces and surrounding unstable mountain slopes is assumed to be a crucial component of this. We hypothesise that the presence of well-developed large lateral moraines along glacier margins serves to reduce this connectivity and therefore reduce the opportunity for glacier-to-rock glacier transition. Understanding these processes is of great importance if we are to better predict the geomorphological evolution of glaciated mountains under conditions of future climate change and the water supply implications that follow.

Acknowledgements

DBJ was funded by the Natural Environment Research Council (Grant No. NE/L002434/1) and the Royal Geographical Society (with IBG) through a Dudley Stamp Memorial Award. The authors wish to thank Dhananjay Regmi and Himalayan Research Expeditions Ltd. for providing organizational support with regards to the fieldwork campaign, and Mahesh Magar, Laxmi Kumar Kulung and Shankar Natshiring are thanked for their invaluable support during data collection. We thank James P. Duffy (University of Exeter) for providing the 3D printed KAP picavet mount, and for his guidance with data processing in Agisoft PhotoScan. The Pleiades image (Fig. 1) was provided by the European Space Agency. Lastly, we acknowledge the detailed and constructive comments of the anonymous reviewers and the editor, which significantly improved the paper.

Declaration of Competing Interest

The authors declare that they have no conflict of interest.

Appendix A. Supplementary data

Supplementary data to this article can be found online at https://doi.org/10.1016/j.gloplacha.2019.102999.

References

KAPshop, 2019. http://www.kapshop.com/, Accessed date: 4 December 2018.

Anderson, R.S., Anderson, L.S., Armstrong, W.H., Rossi, M.W., Crump, S.E., 2018. Glaciation of alpine valleys: the glacier – debris-covered glacier – rock glacier continuum. Geomorphology 311, 127–142.

Arenson, L., Hoelzle, M., Springman, S., 2002. Borehole deformation measurements and internal structure of some rock glaciers in Switzerland. Permafr. Periglac. Process. 13 (2), 117–135.

Azócar, G.F., Brenning, A., 2010. Hydrological and geomorphological significance of rock glaciers in the dry Andes, Chile (27°-33°S). Permafr. Periglac. Process. 21 (1), 42–53.

Ballantyne, C.K., 1982. Aggregate clast form characteristics of deposits near the margins of four glaciers in the Jotunheimen Massif, Norway. Norsk Geografisk Tidsskrift 36 (2), 103–113.

Ballantyne, C.K., 2002. Paraglacial geomorphology. Quat. Sci. Rev. 21 (18), 1935–2017.

Baroni, C., Carton, A., Seppi, R., 2004. Distribution and behaviour of rock glaciers in the Adamello–Presanella Massif (Italian Alps). Permafr. Periglac. Process. 15 (3), 243–259.

Barsch, D., 1977. Nature and importance of mass-wasting by rock glaciers in alpine permafrost environments. Earth Surf. Process. 2 (2–3), 231–245.

Barsch, D., 1987. In: Giardino, J.R., Shroder, J.F., Vitek, J.D. (Eds.), The problem of the ice-cored rock glacier. Rock Glaciers Allen and Unwin, London, pp. 45–54.

Barsch, D., 1988. Rockglaciers. In: Clark, M.J. (Ed.), Advances in Periglacial Geomorphology. Wiley, Chichester, pp. 69–90.

Barsch, D., 1996. Rockglaciers: Indicators for the Present and Former Geoecology in High Mountain Environments. Springer-Verlag, Berlin Heidelberg, Berlin, Germany (331 pp).

Barsch, D., Jakob, M., 1998. Mass transport by active rockglaciers in the Khumbu Himalaya. Geomorphology 26 (1–3), 215–222.

Beniston, M., Farinotti, D., Stoffel, M., Andreassen, L.M., Coppola, E., Eckert, N., Fantini, A., Giacona, F., Hauck, C., Huss, M., Huwald, H., Lehning, M., López-Moreno, J.I., Magnusson, J., Marty, C., Moran-Tejéda, E., Morin, S., Naaim, M., Provenzale, A., Rabatel, A., Six, D., Stötter, J., Strasser, U., Terzago, S., Vincent, C., 2018. The European mountain cryosphere: A review of its current state, trends, and future challenges. Cryosphere 12 (2), 759–794.

Benn, D.I., 2004. Clast morphology. In: Evans, D.J.A., Benn, D.I. (Eds.), A Practical Guide to the Study of Glacial Sediments. Arnold, London, pp. 77–92.

Benn, D.I., Ballantyne, C.K., 1993. The description and representation of particle shape. Earth Surf. Process. Landf. 18 (7), 665–672.

Benn, D.I., Ballantyne, C.K., 1994. Reconstructing the transport history of glacigenic sediments: a new approach based on the co-variance of clast form indices. Sediment. Geol. 91, 215–227.

Benn, D.I., Evans, D.J.A., 2010. Glaciers and Glaciation. Hodder Education, London (802 pp).

Benn, D.I., Owen, L.A., 2002. Himalayan glacial sedimentary environments: a framework for reconstructing and dating the former extent of glaciers in high mountains. Quat. Int. 97-98, 3–25.

Benn, D.I., Kirkbride, M.P., Owen, L.A., Brazier, V., 2004. Glaciated valley landsystems. In: Evans, D.J.A. (Ed.), Glacial Landsystems. Arnold, London, pp. 372–406.

Bennett, M.R., Hambrey, M.J., Huddart, D., 1997. Modification of clast shape in high-Arctic glacial environments. J. Sediment. Res. 67 (3), 550–559.

Berger, J., Krainer, K., Mostler, W., 2004. Dynamics of an active rock glacier (Ötztal Alps, Austria). Quat. Res. 62 (3), 233–242.

Berthling, I., 2011. Beyond confusion: Rock glaciers as cryo-conditioned landforms. Geomorphology 131 (3–4), 98–106.

Bollasina, M., Bertolani, L., Tartari, G., 2002. Meteorological observations at high altitude in the Khumbu Valley, Nepal Himalayas, 1994–1999. Bull. Glaciol. Res. 19, 1–11.

Bosson, J.-B., Lambiel, C., 2016. Internal structure and current evolution of very small debris-covered glacier systems located in alpine permafrost environments. Front. Earth Sci. 4 (39).

Boulton, G.S., 1978. Boulder shapes and grain-size distributions of debris as indicators of transport paths through a glacier and till genesis. Sedimentology 25 (6), 773–799.

Brook, M.S., Lukas, S., 2012. A revised approach to discriminating sediment transport histories in glacigenic sediments in a temperate alpine environment: a case study from Fox Glacier, New Zealand. Earth Surf. Process. Landf. 37 (8), 895–900.

Buchli, T., Merz, K., Zhou, X., Kinzelbach, W., Springman, S.M., 2013. Characterization and monitoring of the Furggwanghorn Rock Glacier, Turtmann Valley, Switzerland: results from 2010 to 2012. Vadose Zone J. 12 (1).

Buchli, T., Kos, A., Limpach, P., Merz, K., Zhou, X., Springman Sarah, M., 2018. Kinematic investigations on the Furggwanghorn rock glacier, Switzerland. Permafr. Periglac. Process. 29 (1), 3–20.

Clark, D.H., Steig, E.J., Potter, J.N., Gillespie, A.R., 1998. Genetic variability of rock glaciers. Geografiska Annaler Ser. A Phys. Geogr. 80 (3–4), 175–182.

Cogley, J.G., Hock, R., Rasmussen, L.A., Arendt, A.A., Bauder, A., Braithwaite, R.J., Jansson, P., Kaser, G., Möller, M., Nicholson, L., Zemp, M., 2011. Glossary of Glacier Mass Balance and Related Terms. UNESCO-IHP, Paris.

Degenhardt Jr., J.J., 2009. Development of tongue-shaped and multilobate rock glaciers in alpine environments – Interpretations from ground penetrating radar surveys. Geomorphology 109 (3–4), 94–107.

Delaloye, R., Lambiel, C., 2005. Evidence of winter ascending air circulation throughout talus slopes and rock glaciers situated in the lower belt of alpine discontinuous permafrost (Swiss Alps). Norsk Geografisk Tidsskrift-Norwegian Journal of Geography 59 (2), 194–203.

Delaloye, R., Perruchoud, E., Avian, M., Kaufmann, V., Bodin, X., Hausmann, H., Ikeda, A., Kääb, A., Kellerer-Pirklbauer, A., Krainer, K., Lambiel, C., Mihajiovic, D., Staub, B., Roer, I., Thibert, E., 2008. Recent interannual variations of rock glacier creep in the European Alps. In: Kane, D.L., Hinkel, K.M. (Eds.), 9th International Conference on Permafrost. Fairbanks, Alaska, pp. 343–348.

Delaloye, R., Lambiel, C., Gärtner-Roer, I., 2010. Overview of rock glacier kinematics research in the Swiss Alps. Geographica Helvetica 65 (2), 135–145.

Delaloye, R., Morard, S., Barboux, C., Abbet, D., Gruber, V., Riedo, M., Gachet, S., 2013. Rapidly moving rock glaciers in Mattertal. In: Graf, C. (Ed.), Jahrestagung der Schweizerischen Geomorphologischen Gesellschaft. Eidg. Forschungsanstalt WSL, St. Niklaus, pp. 21–31.

Duffy, J., Shutler, J., Witt, M., DeBell, L., Anderson, K., 2018. Tracking fine-scale structural changes in coastal dune morphology using kite aerial photography and uncertainty-assessed structure-from-motion photogrammetry. Remote Sens. 10 (9), 1494.

Duguay, M.A., Edmunds, A., Arenson, L.U., Wainstein, P.A., 2015. Quantifying the significance of the hydrological contribution of a rock glacier - a review. In: GEOQuébec 2015: Challenges from North to South, 68th Canadian Geotechnical Conference and 7th Canadian Permafrost Conference, Québec, Canada.

Dusik, J.-M., Leopold, M., Heckmann, T., Haas, F., Hilger, L., Morche, D., Neugirg, F., Becht, M., 2015. Influence of glacier advance on the development of the multipart Riffeltal rock glacier, Central Austrian Alps. Earth Surf. Process. Landf. 40 (7), 965–980.

Emmert, A., Kneisel, C., 2017. Internal structure of two alpine rock glaciers investigated by quasi-3-D electrical resistivity imaging. Cryosphere 11 (2), 841–855.

Eriksen, H.Ø., Rouyet, L., Lauknes, T.R., Berthling, I., Isaksen, K., Hindberg, H., Larsen, Y., Corner, G.D., 2018. Recent acceleration of a rock glacier complex, Ádjet, Norway, documented by 62 years of remote sensing observations. Geophys. Res. Lett. 45, 8314–8323.

Fischer, L., Kääb, A., Huggel, C., Noetzli, J., 2006. Geology, glacier retreat and permafrost degradation as controlling factors of slope instabilities in a high-mountain rock wall: the Monte Rosa east face. Nat. Hazards Earth Syst. Sci. 6 (5), 761–772.

Florentine, C., Skidmore, M., Speece, M., Link, C., Shaw, C.A., 2014. Geophysical analysis of transverse ridges and internal structure at Lone Peak rock glacier, big Sky, Montana, USA. J. Glaciol. 60 (221), 453–462.

Giardino, J.R., Vitek, J.D., 1988. The significance of rock glaciers in the glacial-periglacial landscape continuum. J. Quat. Sci. 3 (1), 97–103.

Glasser, N.F., Harrison, S., Jansson, K.N., 2009. Topographic controls on glacier sediment–landform associations around the temperate North Patagonian Icefield. Quat. Sci. Rev. 28 (25), 2817–2832.

Gorbunov, A.P., Titkov, S.N., Polyakov, V.G., 1992. Dynamics of rock glaciers of the Northern Tien Shan and the Djungar Ala Tau, Kazakhstan. Permafr. Periglac. Process. 3 (1), 29–39.

Graham, D.J., Midgley, N.G., 2000. Graphical representation of particle shape using triangular diagrams: an Excel spreadsheet method. Earth Surf. Process. Landf. 25 (13), 1473–1477.

Guglielmin, M., Ponti, S., Forte, E., 2018. The origins of Antarctic rock glaciers: periglacial or glacial features? Earth Surf. Process. Landf. 43 (7), 1390–1402.

Haeberli, W., 1985. Creep of mountain permafrost: internal structure and flow of alpine rock glaciers. Mitteilungen der Versuchsanstalt für Wasserbau. In: Hydrologie und Glaziologie an der Eidgenössischen Technischen Hochschule Zürich. vol. 77 (Zürich, 142 pp).

Haeberli, W., 2005. Investigating glacier-permafrost relationships in high-mountain areas: Historical background, selected examples and research needs. In: Harris, C., Murton, J.B. (Eds.), Cryospheric Systems: Glaciers and Permafrost. London, Special Publications, Geological Society, pp. 29–37.

Haeberli, W., Hallet, B., Arenson, L., Elconin, R.F., Humlum, O., Kääb, A., Kaufmann, V., Ladanyi, B., Matsuoka, N., Springman, S., Mühll, D.V., 2006. Permafrost creep and rock glacier dynamics. Permafr. Periglac. Process. 17 (3), 189–214.

Hambrey, M.J., Ehrmann, W., 2004. Modification of sediment characteristics during glacial transport in high-alpine catchments: Mount Cook area, New Zealand. Boreas 33 (4), 300–318.

Hambrey, M.J., Glasser, N.F., 2003. Glacial sediments: processes, environments and facies. In: Middleton, G.V. (Ed.), Encyclopedia of Sediments and Sedimentary Rocks. Springer Netherlands, Kluwer, Dordrecht, pp. 316–331.

Hambrey, M.J., Quincey, D.J., Glasser, N.F., Reynolds, J.M., Richardson, S.J., Clemmens, S., 2008. Sedimentological, geomorphological and dynamic context of debris-mantled glaciers, Mount Everest (Sagarmatha) region, Nepal. Quat. Sci. Rev. 27 (25–26), 2361–2389.

Hamilton, S.J., Whalley, W.B., 1995. Rock glacier nomenclature: a re-assessment. Geomorphology 14 (1), 73–80.

Harrison, S., 2009. Climate sensitivity: Implications for the response of geomorphological systems to future climate change. In: Knight, J., Harrison, S. (Eds.), Periglacial and Paraglacial Processes and Environments. Geological Society of London, London, pp. 257–265.

Hartl, L., Fischer, A., Stocker-Waldhuber, M., Abermann, J., 2016. Recent speed-up of an alpine rock glacier: an updated chronology of the kinematics of Outer Hochebenkar rock glacier based on geodetic measurements. Geografiska Annaler Ser. A Phys. Geogr. 98 (2), 129–141.

Hausmann, H., Krainer, K., Brückl, E., Mostler, W., 2007. Internal structure and ice content of Reichenkar rock glacier (Stubai Alps, Austria) assessed by geophysical investigations. Permafr. Periglac. Process. 18 (4), 351–367.

Hausmann, H., Krainer, K., Brückl, E., Ullrich, C., 2012. Internal structure, ice content and dynamics of Ölgrube and Kaiserberg rock glaciers (Ötztal Alps, Austria) determined from geophysical surveys. Austrian J. Earth Sci. 105 (2), 12–31.
Humlum, O., 1996. Origin of rock glaciers: Observations from Mellemfjord, Disko Island, Central West Greenland. Permafr. Periglac. Process. 7 (4), 361–380.
Humlum, O., 2000. The geomorphic significance of rock glaciers: estimates of rock glacier debris volumes and headwall recession rates in West Greenland. Geomorphology 35 (1–2), 41–67.
Ikeda, A., Matsuoka, N., 2006. Pebbly versus bouldery rock glaciers: morphology, structure and processes. Geomorphology 73 (3–4), 279–296.
Ishikawa, M., Watanabe, T., Nakamura, N., 2001. Genetic differences of rock glaciers and the discontinuous mountain permafrost zone in Kanchanjunga Himal, Eastern Nepal. Permafr. Periglac. Process. 12 (3), 243–253.
Iwata, S., 1976. Late Pleistocene and Holocene moraines in the Sagarmatha (Everest) Region, Khumbu Himal: glaciological expedition to Nepal, contribution no. 23. J. Jpn. Soc. Snow Ice 38 (Special), 109–114.
Jakob, M., 1992. Active rock glaciers and the lower limit of discontinuous alpine permafrost, Khumbu Himalaya, Nepal. Permafr. Periglac. Process. 3 (3), 253–256.
Janke, J.R., Regmi, N.R., Giardino, J.R., Vitek, J.D., 2013. Rock glaciers. In: Shroder, J., Giardino, R., Harbor, J. (Eds.), Treatise on Geomorphology. Academic Press, San Diego, CA, pp. 238–273.
Janke, J.R., Ng, S., Bellisario, A., 2017. An inventory and estimate of water stored in firn fields, glaciers, debris-covered glaciers, and rock glaciers in the Aconcagua River Basin, Chile. Geomorphology 296, 142–152.
Jones, D.B., Harrison, S., Anderson, K., Betts, R.A., 2018a. Mountain rock glaciers contain globally significant water stores. Sci. Rep. 8 (1), 2834.
Jones, D.B., Harrison, S., Anderson, K., Selley, H.L., Wood, J.L., Betts, R.A., 2018b. The distribution and hydrological significance of rock glaciers in the Nepalese Himalaya. Glob. Planet. Chang. 160 (Supplement C), 123–142.
Jones, D.B., Harrison, S., Anderson, K., Whalley, W.B., 2019. Rock glaciers and mountain hydrology: A review. Earth Sci. Rev. 193, 66–90.
Kääb, A., Weber, M., 2004. Development of transverse ridges on rock glaciers: field measurements and laboratory experiments. Permafr. Periglac. Process. 15 (4), 379–391.
Kääb, A., Kaufmann, V., Ladstädter, R., Eiken, T., 2003. In: Phillips, M., Springman, S.M., Arenson, L.U. (Eds.), Rock glacier dynamics: Implications from high-resolution measurements of surface velocity fields. vols 1 and 2. Permafrost, pp. 501–506.
Kääb, A., Frauenfelder, R., Roer, I., 2007. On the response of rockglacier creep to surface temperature increase. Glob. Planet. Chang. 56, 172–187.
Kellerer-Pirklbauer, A., Kaufmann, V., 2018. Deglaciation and its impact on permafrost and rock glacier evolution: New insight from two adjacent cirques in Austria. Sci. Total Environ. 621, 1397–1414.
Kellerer-Pirklbauer, A., Rieckh, M., 2016. Monitoring nourishment processes in the rooting zone of an active rock glacier in an alpine environment. Z. Geomorphol. Suppl. 60 (3), 99–121.
Kenner, R., 2019. Geomorphological analysis on the interaction of Alpine glaciers and rock glaciers since the Little Ice Age. Land Degrad. Dev. 30 (5), 580–591.
Kenner, R., Phillips, M., Beutel, J., Hiller, M., Limpach, P., Pointner, E., Volken, M., 2017. Factors controlling velocity variations at short-term, seasonal and multiyear time scales, Ritigraben rock glacier, Western Swiss Alps. Permafr. Periglac. Process. 28 (4), 675–684.
Kirkbride, M.P., 2011. Debris-covered glaciers. In: Singh, V.P., Singh, P., Haritashya, U.K. (Eds.), Encyclopedia of Snow. Ice and Glaciers. Springer Netherlands, Dordrecht, pp. 180–182.
Klaar, M.J., Kidd, C., Malone, E., Bartlett, R., Pinay, G., Chapin, F.S., Milner, A., 2015. Vegetation succession in deglaciated landscapes: implications for sediment and landscape stability. Earth Surf. Process. Landf. 40 (8), 1088–1100.
Knight, J., Harrison, S., 2014. Mountain glacial and paraglacial environments under global climate change: lessons from the past, future directions and policy implications. Geografiska Annaler Ser. A Phys. Geogr. 96 (3), 245–264.
Knight, J., Harrison, S., Jones, D.B., 2019. Rock glaciers and the geomorphological evolution of deglacierizing mountains. Geomorphology 324, 14–24.
Krainer, K., Mostler, W., 2000. Reichenkar rock glacier: a glacier derived debris-ice system in the western Stubai Alps, Austria. Permafr. Periglac. Process. 11 (3), 267–275.
Krainer, K., Mostler, W., 2006. Flow velocities of active rock glaciers in the Austrian Alps. Geografiska Annaler Ser. A Phys. Geogr. 88 (4), 267–280.
Krainer, K., Lang, K., Hausmann, H., 2010. Active rock glaciers at Croda Rossa/Hohe Gaisl, Eastern Dolomites (Alto Adige/South Tyrol, Northern Italy). Geogr. Fis. Din. Quat. 33 (1), 25–36.
Krainer, K., Mussner, L., Behm, M., Hausmann, H., 2012. Multi-disciplinary investigation of an active rock glacier in the Sella Group (Dolomites; northern Italy). Austrian J. Earth Sci. 105 (2), 48–62.
Krainer, K., Bressan, D., Dietre, B., Haas, J.N., Hajdas, I., Lang, K., Mair, V., Nickus, U., Reidl, D., Thies, H., Tonidandel, D., 2015. A 10,300-year-old permafrost core from the active rock glacier Lazaun, southern Ötztal Alps (South Tyrol, northern Italy). Quat. Res. 83 (2), 324–335.
Lambrecht, A., Mayer, C., Hagg, W., Popovnin, V., Rezepkin, A., Lomidze, N., Svanadze, D., 2011. A comparison of glacier melt on debris-covered glaciers in the northern and southern Caucasus. Cryosphere 5 (3), 525–538.
LLC, A., 2017. Photoscan Professional (1.3.5).
Lugon, R., Delaloye, R., Serrano, E., Reynard, E., Lambiel, C., González-Trueba, J.J., 2004. Permafrost and Little Ice Age glacier relationships, Posets Massif, Central Pyrenees, Spain. Permafr. Periglac. Process. 15 (3), 207–220.
Lukas, S., Benn, D.I., Boston, C.M., Brook, M., Coray, S., Evans, D.J.A., Graf, A., Kellerer-Pirklbauer, A., Kirkbride, M.P., Krabbendam, M., Lovell, H., Machiedo, M., Mills, S.C., Nye, K., Reinardy, B.T.I., Ross, F.H., Signer, M., 2013. Clast shape analysis and clast transport paths in glacial environments: a critical review of methods and the role of lithology. Earth Sci. Rev. 121, 96–116.
Małecki, J., Lovell, H., Ewertowski, W., Górski, Ł., Kurczaba, T., Latos, B., Miara, M., Piniarska, D., Płocieniczak, J., Sowada, T., Spiralski, M., Warczachowska, A., Rabatel, A., 2018. The glacial landsystem of a tropical glacier: Charquini Sur, Bolivian Andes. Earth Surf. Process. Landf. 43 (12), 2584–2602.
Martin, H.E., Whalley, W.B., 1987. Rock glaciers. Part 1: Rock glacier morphology: Classification and distribution. Prog. Phys. Geogr. 11 (2), 260–282.
Maurer, H., Huack, C., 2007. Instruments and methods: geophysical imaging of alpine rock glaciers. J. Glaciol. 53 (180).
McCarroll, D., 2016. Simple Statistical Tests for Geography. Chapman and Hall/CRC, Philadelphia, PA, USA (336 pp).
McColl, S.T., 2012. Paraglacial rock-slope stability. Geomorphology 153-154, 1–16.
Messenzehl, K., Meyer, H., Otto, J.-C., Hoffmann, T., Dikau, R., 2017. Regional-scale controls on the spatial activity of rockfalls (Turtmann Valley, Swiss Alps) — A multivariate modeling approach. Geomorphology 287, 29–45.
Micallef, A., Ribó, M., Canals, M., Puig, P., Lastras, G., Tubau, X., 2014. Space-for-time substitution and the evolution of a submarine canyon–channel system in a passive progradational margin. Geomorphology 221, 34–50.
Moncrieff, A.C.M., 1989. Classification of poorly-sorted sedimentary rocks. Sediment. Geol. 65 (1), 191–194.
Monnier, S., Kinnard, C., 2013. Internal structure and composition of a rock glacier in the Andes (upper Choapa valley, Chile) using borehole information and ground-penetrating radar. Ann. Glaciol. 54 (64), 61–72.
Monnier, S., Kinnard, C., 2015a. Internal structure and composition of a rock glacier in the Dry Andes, inferred from ground-penetrating radar data and its artefacts. Permafr. Periglac. Process. 26 (4), 335–346.
Monnier, S., Kinnard, C., 2015b. Reconsidering the glacier to rock glacier transformation problem: new insights from the Central Andes of Chile. Geomorphology 238, 47–55.
Monnier, S., Kinnard, C., 2017. Pluri-decadal (1955–2014) evolution of glacier–rock glacier transitional landforms in the Central Andes of Chile (30–33 °S). Earth Surf. Dynamics 5 (3), 493–509.
Monnier, S., Camerlynck, C., Rejiba, F., Kinnard, C., Galibert, P.-Y., 2013. Evidencing a large body of ice in a rock glacier, Vanoise Massif, Northern French Alps. Geografiska Annaler Ser. A Phys. Geogr. 95 (2), 109–123.
Müller, J., Vieli, A., Gärtner-Roer, I., 2016. Rock glaciers on the run – understanding rock glacier landform evolution and recent changes from numerical flow modeling. Cryosphere 10 (6), 2865–2886.
Nakawo, M., Iwata, S., Watanabe, O., Yoshida, M., 1986. Processes which distribute supraglacial debris on the Khumbu Glacier, Nepal Himalaya. Ann. Glaciol. 8, 129–131.
Outcalt, S.I., Benedict, J.B., 1965. Photo-interpretation of two types of rock glacier in the Colorado Front Range, U.S.A. J. Glaciol. 5 (42), 849–856.
Paine, A.D.M., 1985. 'Ergodic' reasoning in geomorphology:time for a review of the term? Prog. Phys. Geogr. Earth Environ. 9 (1), 1–15.
Pellicciotti, F., Carenzo, M., Bordoy, R., Stoffel, M., 2014. Changes in glaciers in the Swiss Alps and impact on basin hydrology: current state of the art and future research. Sci. Total Environ. 493, 1152–1170.
Petersen, E., Holt, J., Stuurman, C., Levy, J., Nerozzi, S., Paine, J., Larsen, C., Fahnestock, M., 2016. Sourdough Rock Glacier, Alaska: An Analog to Martian Debris-Covered Glaciers, 47th Lunar and Planetary Science Conference.
Potter, N., 1972. Ice-cored rock glacier, Galena Creek, Northern Absaroka Mountains, Wyoming. Geol. Soc. Am. Bull. 83 (10), 3025–3058.
Potter, J.N., Steig, E.J., Clark, D.H., Speece, M.A., Clark, G.M., Updike, A.B., 1998. Galena Creek rock glacier revisited - new observations on an old controversy. Geografiska Annaler Ser. A Phys. Geogr. 80 (3–4), 251–265.
Powers, M.C., 1953. A new roundness scale for sedimentary particles. J. Sediment. Res. 23 (2), 117–119.
Quincey, D.J., Luckman, A., Benn, D., 2009. Quantification of Everest region glacier velocities between 1992 and 2002, using satellite radar interferometry and feature tracking. J. Glaciol. 55 (192), 596–606.
Rangecroft, S., Harrison, S., Anderson, K., Magrath, J., Castel, A., Pacheco, P., 2013. Climate change and water resources in arid mountains: an example from the Bolivian Andes. Ambio 42 (7), 852–863.
Rangecroft, S., Harrison, S., Anderson, K., 2015. Rock glaciers as water stores in the Bolivian Andes: an assessment of their hydrological importance. Arct. Antarct. Alp. Res. 47 (1), 89–98.
Regmi, D., 2008. Rock Glacier distribution and the lower limit of discontinuous mountain permafrost in the Nepal Himalaya. In: Proceedings of the Ninth International Conference on Permafrost, Fairbanks, Alaska, pp. 1475–1480.
Ribolini, A., Chelli, A., Guglielmin, M., Pappalardo, M., 2007. Relationships between glacier and rock glacier in the Maritime Alps, Schiantala Valley, Italy. Quat. Res. 68 (3), 353–363.
Ribolini, A., Guglielmin, M., Fabre, D., Bodin, X., Marchisio, M., Sartini, S., Spagnolo, M., Schoeneich, P., 2010. The internal structure of rock glaciers and recently deglaciated slopes as revealed by geoelectrical tomography: Insights on permafrost and recent glacial evolution in the Central and Western Alps (Italy-France). Quat. Sci. Rev. 29 (3–4), 507–521.
Rowan, A.V., 2017. The 'Little Ice Age' in the Himalaya: a review of glacier advance driven by Northern Hemisphere temperature change. The Holocene 27 (2), 292–308.
Rowan, A.V., Egholm, D.L., Quincey, D.J., Glasser, N.F., 2015. Modelling the feedbacks between mass balance, ice flow and debris transport to predict the response to climate change of debris-covered glaciers in the Himalaya. Earth Planet. Sci. Lett. 430, 427–438.
Salerno, F., Guyennon, N., Thakuri, S., Viviano, G., Romano, E., Vuillermoz, E., Cristofanelli, P., Stocchi, P., Agrillo, G., Ma, Y., Tartari, G., 2015. Weak precipitation,

warm winters and springs impact glaciers of south slopes of Mt. Everest (central Himalaya) in the last 2 decades (1994-2013). Cryosphere 9 (3), 1229–1247.
Scherler, D., Bookhagen, B., Strecker, M.R., 2011. Spatially variable response of Himalayan glaciers to climate change affected by debris cover. Nat. Geosci. 4 (3), 156–159.
Searle, M.P., Simpson, R.L., Law, R.D., Parrish, R.R., Waters, D.J., 2003. The structural geometry, metamorphic and magmatic evolution of the Everest massif, High Himalaya of Nepal–South Tibet. J. Geol. Soc. 160 (3), 345.
Seppi, R., Zanoner, T., Carton, A., Bondesan, A., Francese, R., Carturan, L., Zumiani, M., Giorgi, M., Ninfo, A., 2015. Current transition from glacial to periglacial processes in the Dolomites (South-Eastern Alps). Geomorphology 228, 71–86.
Serrano, E., Juan de Sanjose, J., Jose Gonzalez-Trueba, J., 2010. Rock glacier dynamics in marginal periglacial environments. Earth Surf. Process. Landf. 35 (11), 1302–1314.
Shroder, J.F., Bishop, M.P., Copland, L., Sloan, V.F., 2000. Debris-covered glaciers and rock glaciers in the Nanga Parbat Himalaya, Pakistan. Geografiska Annaler Ser. A Phys. Geogr. 82 (1), 17–31.
Smith, M.W., Carrivick, J.L., Quincey, D.J., 2016. Structure from motion photogrammetry in physical geography. Prog. Phys. Geogr. 40 (2), 247–275.
Sneed, E.D., Folk, R.L., 1958. Pebbles in the lower Colorado River, Texas a study in particle morphogenesis. J. Geol. 66 (2), 114–150.
Sorg, A., Kääb, A., Roesch, A., Bigler, C., Stoffel, M., 2015. Contrasting responses of Central Asian rock glaciers to global warming. Sci. Rep. 5, 8228.
Wahrhaftig, C., Cox, A., 1959. Rock glaciers in the Alaska range. Geol. Soc. Am. Bull. 70 (4), 383–436.
Watson, C.S., Quincey, D.J., Carrivick, J.L., Smith, M.W., 2016. The dynamics of supraglacial ponds in the Everest region, central Himalaya. Glob. Planet. Chang. 142, 14–27.
Watson, C.S., Quincey, D.J., Carrivick, J.L., Smith, M.W., Rowan, A.V., Richardson, R., 2018. Heterogeneous water storage and thermal regime of supraglacial ponds on debris-covered glaciers. Earth Surf. Process. Landf. 43 (1), 229–241.
Westoby, M.J., Brasington, J., Glasser, N.F., Hambrey, M.J., Reynolds, J.M., 2012. 'Structure-from-Motion' photogrammetry: A low-cost, effective tool for geoscience applications. Geomorphology 179, 300–314.
Whalley, W.B., 1974. Origin of rock glaciers. J. Glaciol. 13 (68), 323–324.
Whalley, W.B., Azizi, F., 2003. Rock glaciers and protalus landforms: analogous forms and ice sources on Earth and Mars. J. Geophys. Res. Planet. 108 (E4).
Whalley, W.B., Martin, H.E., 1992. Rock glaciers: II models and mechanisms. Prog. Phys. Geogr. 16 (2), 127–186.
White, S.E., 1976. Rock glaciers and block fields, review and new data. Quat. Res. 6 (1), 77–97.
Wigmore, O., Mark, B., 2018. High altitude kite mapping: evaluation of kite aerial photography (KAP) and structure from motion digital elevation models in the Peruvian Andes. Int. J. Remote Sens. 39 (15–16), 4995–5015.
Wirz, V., Gruber, S., Purves, R.S., Beutel, J., Gärtner-Roer, I., Gubler, S., Vieli, A., 2016. Short-term velocity variations at three rock glaciers and their relationship with meteorological conditions. Earth Surf. Dynamics 4 (1), 103–123.